



Long-term plankton and environmental monitoring dataset from the Marine Protected Area of the Iroise Marine Natural Park (2010-2023) in the Iroise Sea, North Atlantic

Laetitia Drago¹, Caroline Cailliau², Patrick Pouline², Beatriz Beker³, Laëtitia Jalabert⁴, Jean-Baptiste Romagnan⁵, Sakina-Dorothee Ayata^{1,6}

¹Sorbonne Université, MNHN, CNRS, IRD, Laboratoire d'Océanographie et du Climat : Expérimentations et Approches Numériques, LOCEAN, F-75005 Paris, France

²Parc naturel marin d'Iroise, Office Français de la Biodiversité, Le Conquet, France

15 ³Laboratoire des Sciences de l'Environnement MARin (LEMAR), UMR 6539, Université de Bretagne Occidentale, Plouzané, France

⁴Sorbonne Université, CNRS, Institut de la Mer de Villefranche, IMEV, F-06230, Villefranche-sur-Mer, France

⁵DECOD, L'Institut Agro, IFREMER, INRAE, 44000, Nantes, France

⁶Institut Universitaire de France, F-75005 Paris, France

15 *Correspondence to:* Laetitia Drago (laetitia.drago@locean.ipsl.fr) and Sakina-Dorothee Ayata (sakina-dorothee.ayata@locean.ipsl.fr)

Abstract. This data paper presents a long-term monitoring dataset of phytoplankton (2010-2022) and zooplankton (2010-2023) communities, as well as associated environmental parameters (2010-2023), from the Iroise Marine Natural Park, Iroise Sea, North Atlantic, France's first Marine Protected Area. The dataset combines traditional microscopy-based phytoplankton counts with zooplankton data (abundances) obtained from digitized images using the ZooScan imaging system, along with surface and bottom temperature and salinity measurements. Sampling was conducted seasonally along two main transects and three coastal stations, capturing both spatial and temporal dynamics of plankton communities. Phytoplankton was identified at the species level by the same taxonomist during all the time-series (573 taxa in total). From their individual images, zooplankton was automatically sorted into 103 taxonomic and morphological groups, validated by an expert, and compiled into a data table allowing both community and individual approaches using abundances and biovolumes at both individual and community levels. Individual zooplankton images have also been made available for further morphometric analyses. This 14-year long, spatially and temporally resolved zooplankton imaging dataset is part of an ongoing effort to enhance the availability of zooplankton imaging data, locally and globally. This, as a whole dataset, can be used to study the influence of coastal-offshore environmental gradients on marine plankton biodiversity patterns, especially in protected waters at the intersection of the English Channel and the Atlantic Ocean, in a region characterized by the presence of the Ushant front.

1 Introduction

Planktonic organisms play a pivotal role in marine and freshwater ecosystems (Grigoratou, in press). They are key contributors to the biological carbon pump, with phytoplankton fixing atmospheric CO₂ (Simon et al., 2008) and zooplankton exporting this carbon through the sinking of molts and carcasses, the production of fecal pellets and diel vertical migration (Steinberg and Landry, 2017). As the foundation of aquatic food webs (Ikeda, 1985), these organisms sustain diverse marine life, from marine mammals and birds to commercial fish species (Chavez et al., 2008; Frederiksen et al., 2006), with substantial economic implications (Richardson et al., 2009; van der Lingen et al., 2006).



40 Long-term monitoring of planktonic communities through time-series datasets has proven invaluable for understanding
 marine ecosystem dynamics. The number of sustained observation programs has grown significantly in past decades,
 spanning diverse environments from coastal monitoring stations to open ocean sites (Batchelder et al., 2012; Berline et al.,
 2012; Grandremy et al., 2024). These datasets have revealed crucial insights into planktonic community dynamics across
 multiple temporal and spatial scales, though continued expansion of such monitoring efforts remains important for
 45 comprehensive ecosystem understanding (Jonkers et al., 2022; Pitois and Yebra, 2022).

Imaging technologies have emerged as powerful tools for studying planktonic communities, enabling high-throughput
 analysis of both taxonomic and trait-based characteristics (Irisson et al., 2022; Orenstein et al., 2022). Datasets originating
 from these technologies are providing unprecedented views into the diversity and distribution of zooplankton (Panaïotis et
 50 al., 2023; Perhirin et al., 2023; Vilgrain et al., 2021) and phytoplankton (Bolaños et al., 2020; Kenitz et al., 2020; Sonnet et
 al., 2022). These imaging approaches allow for rapid processing of large sample volumes while capturing detailed
 morphological information, facilitating both traditional taxonomic identification and novel trait-based analyses (Irisson et al.,
 2022; Orenstein et al., 2022). Indeed, although studies have traditionally focused on the taxonomic diversity of plankton,
 there is a growing recognition of the relevance of trait-based approaches, which can offer deeper insights into ecosystem
 55 functioning and community responses to environmental changes (Kjørboe et al., 2018; Litchman et al., 2013; Martini et al.,
 2021). Traits such as body size and shape, feeding mode, and motility can provide a more mechanistic understanding of
 plankton ecology and their role in biogeochemical processes (Buitenhuis et al., 2013; Litchman et al., 2015).

Despite these technological advances, significant challenges remain in making plankton datasets widely accessible and
 60 useful for the broader scientific community. The need for standardized, well-documented, and openly accessible datasets is
 increasingly critical, particularly for supporting long-term ecological monitoring and modeling efforts. Following FAIR
 principles (Findable, Accessible, Interoperable, and Reusable) defined by Wilkinson et al. (2016), modern plankton datasets
 must include comprehensive metadata and standardized protocols to ensure their utility across different research applications
 (Titocci et al., 2025). Recently, several plankton datasets have been published following the FAIR principle (Acri et al.,
 65 2020; Devreker et al., 2024; Dugenne et al., 2024; Grandremy et al., 2024). Following this trend, we present here a long-term
 dataset (2010-2024) from the Iroise Marine Natural Park, France's first Marine Protected Area (MPA). The dataset includes a
 phytoplankton time-series based on microscopy counts (conducted by a single taxonomist throughout the study period) and a
 zooplankton dataset that comprises digitized images obtained by the ZooScan imaging system and associated abundances.
 Both datasets are accompanied by contextual environmental variables (temperature, salinity). These datasets will contribute
 70 to a better understanding of plankton dynamics in protected Atlantic waters, while serving as examples of how traditional
 and modern approaches could be effectively combined and shared to support observational studies, monitoring surveys, and
 modeling efforts (Holland et al., 2025).



2 Study site

The Iroise Marine Natural Park (“Parc Naturel Marin d’Iroise” in French; <https://parc-marin-iroise.fr/>), established in 2007 as the first French Marine Protected Area (MPA), spans 3,550 km² off the western coast of Brittany. Managed by the French Biodiversity Agency (Office Français de la Biodiversité, OFB), this MPA encompasses the Iroise Sea, a unique ecosystem located at the intersection of the English Channel and the Atlantic Ocean. The MPA’s monitoring activities align with two major European directives: the Water Framework Directive (WFD/DCE) for coastal waters and the Marine Strategy Framework Directive (MSFD/DCSMM) which aims to achieve Good Environmental Status of marine waters. As Essential Ocean Variables (EOVs), plankton communities are key indicators within the MSFD framework, providing crucial information about ecosystem health and food web dynamics (Batten et al., 2019). Their monitoring is particularly relevant for MPAs like the Iroise Marine Natural Park, as the rapid responses of these organisms to environmental changes can serve as early warning signals of ecosystem shifts. It is also particularly relevant for fisheries (Benedetti et al., 2019; Berthou et al., 2010; Duhamel et al., 2011), as small pelagic fishes like sardines (*Sardina pilchardus*) feed on plankton (Garrido et al., 2008). The Iroise area also serves as a natural laboratory due to its complex oceanography, particularly the seasonal Ushant thermal front (Le Boyer et al., 2009; Pingree et al., 1975) which can act as a barrier for the dispersal of planktonic organisms between the Lusitanian biogeographical province in the South and the Boreal biogeographical province in the North (Ayata et al., 2010). This front, along with an inner front and distinct surface-bottom dynamics, creates diverse habitats that support rich plankton communities and overall marine biodiversity (Cadier et al., 2017; Ramond et al., 2021; Schultes et al., 2013). As a result, the Iroise Sea also holds significant economic and cultural importance for France's sardine fishery. A substantial portion of France's sardine catches come from this region and adjacent waters, with the port of Douarnenez serving as a historic sardine fishing hub and exemplifying a traditional sardine fishing community (Le Floc’h et al., 2020). Beyond its ecological and conservation value, this economic and cultural heritage contributed to the creation of the Iroise Marine Natural Park as the first Marine Protected Area in France.

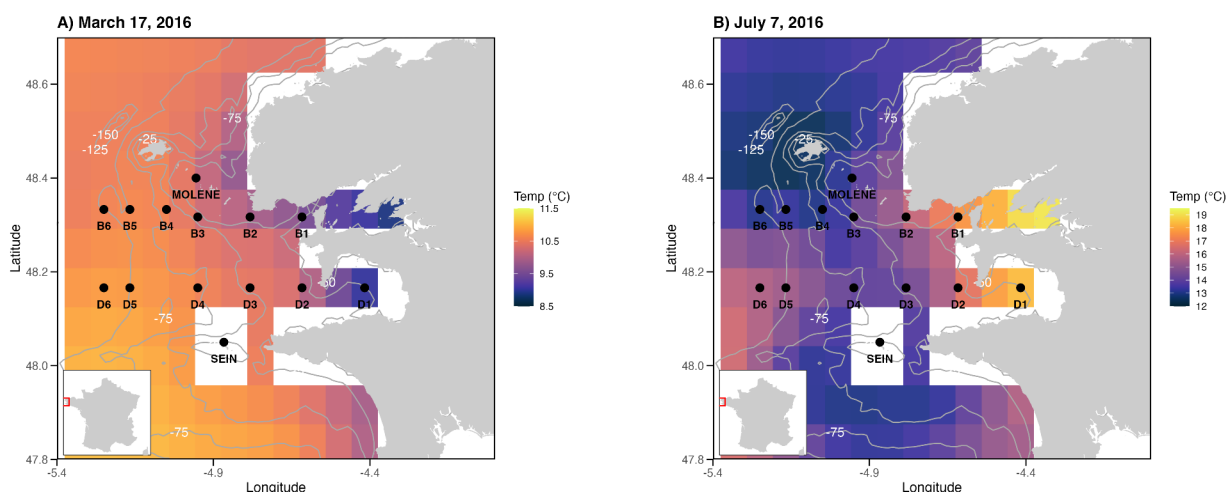
3 Material and methods

3.1 Sampling

Plankton community sampling in the Iroise Marine Natural Park was conducted through regular monitoring cruises operated by the OFB-PNMI on board the vessel N/O *Albert Lucas* for the years 2011 and 2012, and on board the *ValBelle* PM 509 vessel in the North and the *Augustine* PM 510 vessel in the South between 2013 and 2024. Sampling design (Fig. 1; Table 1) included two parallel transects following a coastal-offshore gradient, as well as three coastal stations (Molène, Sein and Douarnenez). The northern transect B (offshore Brest) included seven stations (B1 to B7 from coast to offshore) and extended slightly further than the southern transect D (offshore Douarnenez), which comprised six stations (D1 to D6, with D1 being more eastward than B1). Transect cruises were scheduled to capture seasonal variations, with sampling conducted



in late spring, mid-summer, and mid-autumn, covering three of the four seasons until 2017 (See Supplementary Table 1).
105 Since that year, the sampling frequency has increased from three to four times per year (see Supplementary Table 1 for details). For the three coastal stations, phytoplankton were sampled every two weeks and zooplankton every month (Supplementary Table 2). The highly variable weather of the region occasionally prevented comprehensive sampling of hydrobiological variables and plankton at all stations. The Douarnenez station being the same as the station D1, they are treated together in this paper.



110

Figure 1: Sampling zone in the Iroise Marine Natural Park with northern transect B (stations B1 to B7 from coast to open ocean), southern transect D (stations D1 to D6 from coast to open ocean) and coastal stations Molène, Sein and Douarnenez (D1). Background temperature data used in the figure corresponds to data obtained at 12:30 pm on March 17, 2016 and July 7, 2016, coinciding with sampling days. This data was downloaded from Copernicus Marine Services using
115 the product [“European North West Shelf/Iberia Biscay Irish Seas - High Resolution L4 Sea Surface Temperature Reprocessed” \(CMEMS, 2024\).](#)

Water samples were collected bi-monthly by the Iroise Marine Natural Park technical personnel using a 5 L Niskin bottle following the Service d’Observation en Milieu Littoral (SOMLIT) (Cocquempot et al., 2019) and Institut Universitaire
120 Européen de la Mer (IUEM) protocols. Samples were promptly divided into flasks and delivered to IDHESA laboratory (Brest site accreditation no. 1-1827 and Quimper site accreditation no. 1-1828) for analysis of temperature and salinity.

**Table 1: Coordinates and sampling depth of the stations on the two transects and the coastal stations. For the transect stations, the sampling is done both at the subsurface and at depth. For the coastal stations (Molène, Sein,
125 Douarnenez), the sampling is only done at the subsurface.**



Station	Lat.(°N)	Long.(°W)	Bathymetry (m)	Bottom sampling depth (m)
B1	48°19,02	04°37,02	25	20
B2	48°19,02	04°46,98	24	20
B3	48°19,02	04°57,00	18	15
B4	48°19,98	05°3,00	50	45
B5	48°19,98	05°10,02	100	80
B6	48°19,98	05°15,00	111	90
B7	48°19,98	05°25,02	118	90
D1/Douarnenez	48°9,96	04°25,02	26	20
D2	48°9,96	04°37,02	38	30
D3	48°9,96	04°46,98	51	45
D4	48°9,96	04°57,00	87	75
D5	48°9,96	05°10,02	100	90
D6	48°9,96	05°15,00	113	90
Molène	48° 23,600'	04° 57,20'	15	No bottom sampling
Sein	48° 02,600'	04° 52,00'	41	

3.1.1 Hydrological data acquisition

Salinity and temperature were measured at each station with a WTW probe (Cond 1970i) equipped with a standard conductivity measuring cell (TetraCon 325/C), at the subsurface (approximately 1 m depth) and 1 m above the bottom. From 2017, salinity and temperature were also measured using a CTD sensor (NKE MP7 sensor).

130 3.1.2 Phytoplankton sampling

For the transect stations, phytoplankton was sampled bi-monthly both at sub-surface and above the bottom (before 2016) or at 15 m depth (since 2016). In coastal stations, it was sampled bi-monthly at sub-surface only. Samples were preserved in 250 ml glass flasks with 1 ml of Lugol's solution and stored at ambient temperature in darkness. The annual number of phytoplankton samples varied annually (from 12 in 2010 and 2014 to 97 in 2017), with reduced winter sampling due to weather conditions. The study collected 785 phytoplankton samples in total (Fig. 2). Phytoplankton sampling effort increased notably from 2010 to 2017 (Fig. 2), with peaks in sampling effort occurring in 2013 and 2015 (approximately 80 samples per year) and between 2017 and 2019 (between 83 samples for 2018 and 97 samples for 2017). The sampling effort then gradually decreased to about 50 samples in 2022.



140 **Figure 2: Temporal distribution of phytoplankton and zooplankton sampling effort from 2010 to 2023.** The stacked
 bars represent the number of samples collected per season (Fall, Spring, Summer, Winter) for each year. Upper panel shows
 phytoplankton sampling frequency (total number of phytoplankton samples = 785) while the lower panel shows zooplankton
 sampling frequency (total number of zooplankton samples = 650). Note that phytoplankton sampling was reduced in 2014
 while no zooplankton samples were collected that year. Indeed, the funding agency needed to be reassured on the fact that
 145 collecting this data was useful given its cost. Publishing such datasets in open access is then a way to reassure the funders
 that collecting such datasets is indeed useful for the scientific community.

3.1.3 Zooplankton sampling

Zooplankton was sampled using a 200 μm mesh size WP2 plankton net with a 57 cm opening diameter. At the sampling site,
 150 the WP2 net was deployed to a maximum depth of 5 m above the sediment. The net was then retrieved at a speed of 1 m/s. In



the absence of a flow meter, the filtered volume was estimated by multiplying the net's mouth area by the length of cable deployed. This calculation assumed consistent and adequate filtering efficiency across all sampling events. The collected zooplanktonic organisms were transferred into a 250 ml double-sealed polypropylene flask and preserved by adding buffered formaldehyde (4%) in a 1:3 sample-to-formaldehyde ratio. The annual number of zooplankton samples from 16 samples in 2010 (the first year of sampling) to 68 samples in 2013, reflecting variations in sampling strategy and weather conditions (Fig. 2). In total, 650 zooplankton samples were collected.

3.2 Plankton identification and processing

3.2.1 Phytoplankton identification

Phytoplanktonic organisms were then counted under a microscope by Beatriz Beker, who is a specialized phytoplankton taxonomist from the French network RESOMAR (Réseau des Stations et Observatoires Marins). She has been consistently performing these analyses from 2010 to present. Microscopic analysis was performed on 50 ml subsamples following concentration using Utermöhl settling chambers (Hasle, 1978). Enumeration was conducted using phase contrast microscopy (Wild M40 inverted microscope) along diametrical transects at 300× or 600× magnification. Following Lund et al. (1958), the entire chamber surface was analyzed when warranted by specimen size or abundance. Taxonomic identification was performed to the lowest feasible level, with diatoms, dinoflagellates, and nanophytoplankton generally identified to genus and species. The employed methodology precluded identification and measurement of picophytoplankton.

3.2.2 Zooplankton digitization and identification

Zooplankton samples were digitized using the ZooScan imaging system (Gorsky et al., 2010), a waterproof flatbed scanner that generates high-resolution (2400 dpi, pixel size: 10.56 µm) 16-bit grayscale images. All steps from digitization to identification were carried out at the EMBRC Quantitative Imaging Platform (PIQv) of the Institut de la Mer de Villefranche (<https://sites.google.com/view/piqv/>). Prior to scanning, samples underwent a size-based separation process to prevent the underrepresentation of larger, less abundant organisms that might otherwise be lost in the fractionning process. This involved filtering the samples through a 1000 µm mesh, creating two distinct size classes: one for organisms exceeding 1 mm (large fraction) and another for those below this threshold (small fraction). A 100 µm mesh sieve, smaller than the net mesh size, was also used to prevent sample loss. Each size fraction was then fractionated using a Motoda plankton splitter (Motoda, 1959) to reduce the number of organisms per scan and limit as much as possible objects overlap, following recommendations by Vandromme et al. (2012) and Jalabert et al. (2024).



3.2.3 Zooplankton image processing

ZooScan images were processed using the ZooProcess software (Gorsky et al., 2010). The ZooScan captures 16-bit grayscale images of both the background and plankton samples, which are then converted to 8-bit. This conversion maps pixel values from 0 (black) to 255 (white) while preserving the meaningful grey range of the original image.

This normalization ensures comparability across different ZooScans without compromising identification accuracy, as the 8-bit resolution still exceeds the opacity variations found in preserved plankton. Next, a background image was subtracted from each sample image to create a nearly white background.

Finally, particle processing was performed, where objects were segmented and extracted based on two thresholds: a gray-level intensity of 243 and a minimum Equivalent Spherical Diameter (ESD) of 300 μm . The final output includes a table with 42 measurements (such as area, major and minor axes, grey level, and transparency...) (<https://zenodo.org/records/14704251>) along with individual Regions of Interest (ROIs) for each detected object.

The digitized objects were then imported into the EcoTaxa web platform (Picheral et al., 2017, <https://ecotaxa.obs-vlfr.fr/>), where supervised learning algorithms performed initial taxonomic classification, followed by a manual validation by human experts from the PIQv (Irisson et al., 2022). Organisms were categorized into 103 biological categories, excluding detritus, bubbles, and other scanning artifacts (Fig. 3).

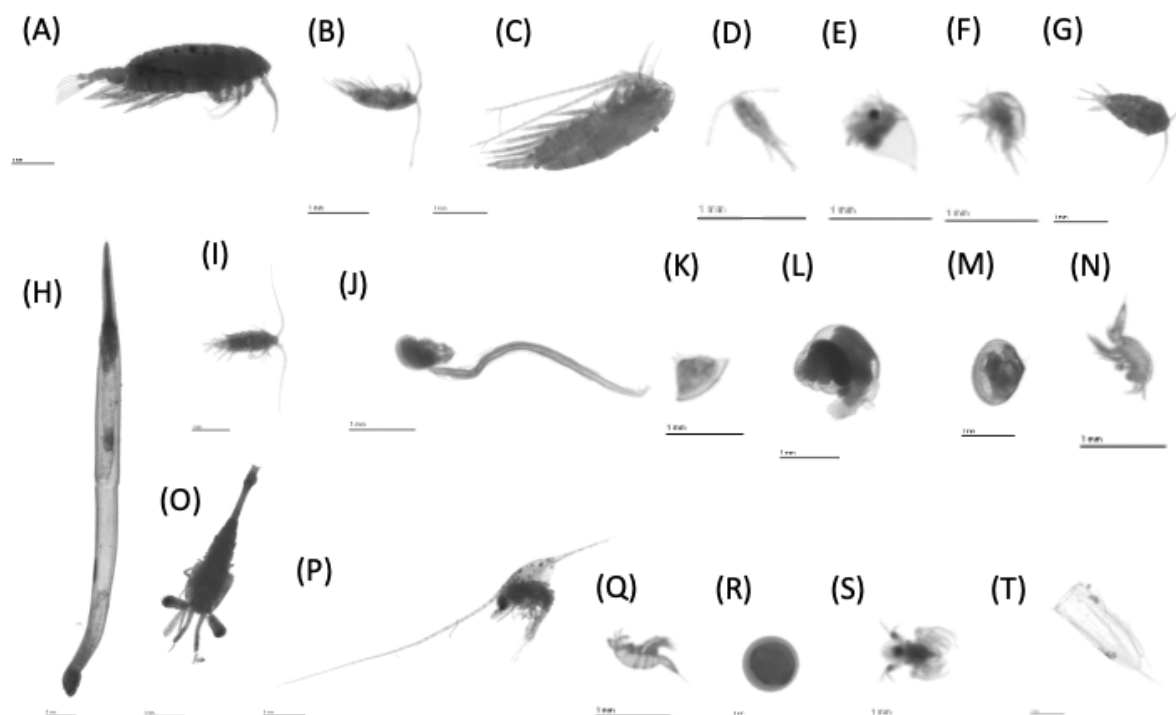


Figure 3: Examples of planktonic organisms imaged by the Zooscan for the 20 most abundant taxa. (A) Calanoida, (B) Acartiidae, (C) Calanidae, (D) Oithonidae, (E) Evadne, (F) nauplii<Cirripedia, (G) Temoridae, (H) Chaetognatha, (I) Acartiidae, (J) Acartiidae, (K) Acartiidae, (L) Acartiidae, (M) Acartiidae, (N) Acartiidae, (O) Acartiidae, (P) Acartiidae, (Q) Acartiidae, (R) Acartiidae, (S) Acartiidae, (T) Acartiidae.



Centropagidae, (J) Oikopleuridae, (J) Centropagidae, (K) cyphonaute, (L) Limacinidae, (M) Bivalvia<Mollusca, (N) Oncaeidae, (O) Eumalacostraca, (P) larvae<Porcellanidae, (Q) Harpacticoida, (R) egg<other, (S) Podon, (T) nectophore<Diphyidae. Note that a scale bar of 1 mm is represented in each image for comparison.

200 For samples collected between 2018 and 2023, experts from the PIQv reviewed and validated the classified objects, making corrections where necessary, serving as a strong quality assurance indicator. This validation process ensured taxonomic homogenization across projects during these years. This dual approach - combining efficient computational methods with expert biological knowledge - optimizes the balance between processing speed and taxonomic precision. It allows for the reliable analysis of large-scale plankton datasets while maintaining high standards of scientific rigor.

205 3.3 Data processing

3.3.1 Environmental data processing

For both salinity and temperature, after removing abnormal data (e.g., negative salinity), the data was binned on a 1 m depth bin interpolated on a 1 m vertical resolution.

3.3.2 Phytoplankton data processing

210 The 785 phytoplankton samples contained 573 unique taxa distributed across 9 taxonomic ranks from Phylum to Variety level, with the majority represented at the genus (164 taxa) and species (359 taxa) levels (Table 2).

The Douarnenez station, being sampled at the same location as the D1 station from the southern transect, was redesignated as D1 while retaining a "Douarnenez" tag for subsequent analyses. Based on the sampling month, data were grouped by season: winter (December, January, February), spring (March, April, May), summer (June, July, August), and fall
 215 (September, October, November). Proportions of each taxon were computed at various taxonomic levels to examine taxa distribution on both seasonal and annual scales.

Table 2: Number of unique taxa and occurrences across taxonomic ranks in marine phytoplankton samples from 2010 to 2022.

Taxonomic rank	Number	Occurrence
Phylum	2	2476
Forma	7	8666
Class	12	14856
Subclass	2	2476
Order	10	12380
Family	4	4952
Genus	168	207984



Species	359	444442
Variety	5	6190

3.3.3. Zooplankton data processing

220 Zooplankton imaging data was downloaded from Ecotaxa projects (see Supplementary Table 3 for the detailed references of Ecotaxa projects), resulting in a dataset containing a total of 832,830 individual images of zooplankton organisms. Abundances (in ind. m⁻³) were computed using the subsampling ratios (column `acq_sub_part` of the Ecotaxa table) for both the large (`acq1`) and small (`acq2`) size fractions (see methods section 3.2.2.). They were then normalized by total sampled seawater volumes (column `sample_tot_vol` of the Ecotaxa table) following Eq. (1):

$$225 \quad Abundance_{taxon} = \frac{\left(n_{taxon_{acq1}} \times acq_{subpart_{acq1}}\right) + \left(n_{taxon_{acq2}} \times acq_{subpart_{acq2}}\right)}{sample \ total \ volume} \quad (1)$$

where n is the number of individuals for the corresponding taxon.

The area (in pixels) obtained through ZooProcess image analysis was converted to mm² using the converting column from the Ecotaxa table called `process_particle_pixel_size_mm`. This allowed to compute the equivalent spherical diameter (ESD, in mm) following Eq. (2):

$$ESD = 2 \times \sqrt{\frac{Area}{\pi}} \quad (2)$$

To compute the biovolume (in mm³) of each organism, we used the spheroid method based on area measurements following Eq. (3):

$$Spheroid = \frac{4}{3} \times \pi \times \left(\frac{ESD}{2}\right)^3 \quad (3)$$

235 This approach was chosen to avoid errors that can occur with ellipse fitting, especially for organisms with irregular shapes or protruding appendages. Area measurements, obtained through ZooProcess image analysis, provide a more consistent basis for estimating biovolume across diverse plankton morphologies (Drago et al., 2022).

The image data were thereafter grouped into 17 broader taxonomic groups (see Table 3).

240 **Table 3: Names of the taxonomic groups of the zooplankton dataset according to the Ecotaxa annotation (column “annotation_category”), the regroupment proposed in this paper (column “groups”) as well as the associated number of images and their relative frequencies across the complete dataset.**



annotation_category	groups	count	%	annotation_category	groups	count	%
Calanoida	Copepoda	163503	27,43	bract<Diphyidae	Cnidaria	444	0,07
Acartiidae	Copepoda	77012	12,92	Clione	Mollusca	432	0,07
Calanidae	Copepoda	41894	7,03	Copepoda<Maxillopoda	Copepoda	380	0,06
Oithonidae	Copepoda	34166	5,73	protozoa<Mysida	Malacostraca	329	0,06
Evadne	Branchiopoda	23131	3,88	nectophore<Physonectae	Cnidaria	323	0,05
nauplii<Cirripedia	Mollusca	22933	3,85	Tomopteridae	Annelida	285	0,05
Temoridae	Copepoda	20729	3,48	veliger		189	0,03
Chaetognatha	Chaetognatha	20474	3,43	Amphipoda	Malacostraca	168	0,03
Centropagidae	Copepoda	18446	3,09	Foraminifera	Harosa	159	0,03
Oikopleuridae	Appendicularia	18080	3,03	Ophiurida	Echinodermata	141	0,02
cyphonaute	Bryozoa	14435	2,42	Metridia	Copepoda	130	0,02
Limacinidae	Mollusca	13896	2,33	Liriope<Geryoniidae	Cnidaria	117	0,02
Bivalvia<Mollusca	Mollusca	12408	2,08	juvenile<Salpida		100	0,02
Oncaeidae	Copepoda	9994	1,68	Leptothecata	Cnidaria	99	0,02
Eumalacostraca	Malacostraca	9341	1,57	Aglaura	Cnidaria	98	0,02
larvae<Porcellanidae	Decapoda	8569	1,44	Atlanta	Mollusca	92	0,02
Harpacticoida	Copepoda	6567	1,1	Mollusca	Mollusca	88	0,01
egg<other		5928	0,99	Pontellidae	Copepoda	75	0,01
Podon	Branchiopoda	5910	0,99	Monstrilloida	Copepoda	61	0,01
nectophore<Diphyidae	Cnidaria	5437	0,91	body<megalopa	Decapoda	60	0,01
Hydrozoa	Cnidaria	4684	0,79	Harosa	Harosa	59	0,01
nauplii<Crustacea		4388	0,74	Ctenophora<Metazoa	Ctenophora	58	0,01
Ophiuroidea	Echinodermata	3107	0,52	Phoronida		49	0,01
Corycaeidae	Copepoda	2987	0,5	invisible membrane<egg	Fish	48	0,01
cypris	Mollusca	2918	0,49	Insecta		47	0,01
Metridinidae	Copepoda	2821	0,47	Branchiostoma		35	0,01
zoea<Brachyura	Decapoda	2771	0,46	Echinoidea	Echinodermata	33	0,01
calyptopsis<Euphausiacea	Euphausiacea	2657	0,45	larvae<Crustacea		33	0,01
egg<Sardina pilchardus	Fish	2535	0,43	larvae<Squillidae	Malacostraca	30	0,01
Doliolida	Thaliacea	2426	0,41	Gymnosomata	Mollusca	18	< 0,01
cirrus	Mollusca	2226	0,37	Sapphirinidae	Copepoda	16	< 0,01
Obelia	Cnidaria	2170	0,36	phyllsoma	Decapoda	14	< 0,01
Gammaridea	Malacostraca	2130	0,36	Scyphozoa	Cnidaria	13	< 0,01
gonophore<Diphyidae	Cnidaria	2114	0,35	Isopoda	Malacostraca	10	< 0,01
Euchaetidae	Copepoda	1933	0,32	Creseidae	Mollusca	9	< 0,01
egg<Actinopterygii	Fish	1894	0,32	Ostracoda		9	< 0,01
Penilia	Branchiopoda	1860	0,31	Siphonophorae	Cnidaria	9	< 0,01
Fritillariidae	Appendicularia	1743	0,29	chain<Salpida		9	< 0,01
Candaciidae	Copepoda	1544	0,26	Cephalopoda	Mollusca	6	< 0,01
pluteus<Ophiuroidea	Echinodermata	1500	0,25	ephyra<Scyphozoa	Cnidaria	6	< 0,01
Hyperidea	Malacostraca	1204	0,2	Cavolinia inflexa	Mollusca	5	< 0,01
zoea<Galatheidae	Decapoda	1040	0,17	Crustacea		5	< 0,01
eudoxie<Diphyidae	Cnidaria	1026	0,17	Caprellidae	Malacostraca	3	< 0,01
Annelida	Annelida	807	0,14	Cumacea	Cumacea	3	< 0,01
pluteus<Echinoidea	Echinodermata	722	0,12	Pycnogonida		2	< 0,01
Salpida	Thaliacea	718	0,12	Abylidae	Cnidaria	1	< 0,01
Sertulariidae	Cnidaria	675	0,11	Acantharea	Harosa	1	< 0,01
larvae<Annelida	Annelida	626	0,11	Aequorea	Cnidaria	1	< 0,01
Actinopterygii	Fish	624	0,1	Cirripedia		1	< 0,01
Echinodermata	Echinodermata	572	0,1	Cyclopoida	Copepoda	1	< 0,01
megalopa<Brachyura		498	0,08	Ophiothrix	Echinodermata	1	< 0,01
				Physonectae	Cnidaria	1	< 0,01



4 Data quality control

245 Multiple quality control procedures were implemented throughout data collection, processing, and analysis to ensure data reliability and consistency. These procedures covered environmental parameters, phytoplankton identification, and zooplankton classification.

For environmental parameters, systematic quality checks were performed on temperature and salinity measurements. Abnormal values, such as negative salinity readings, were removed from the dataset. The remaining data underwent binning
 250 on 1-meter depth intervals with interpolation at 1-meter vertical resolution. Additional quality control included outlier detection and removal based on a 0.001 quantile threshold.

Phytoplankton identification quality was maintained through taxonomic consistency, with all microscopic analyses performed by a single specialized taxonomist (Beatriz Beker from the French network RESOMAR) throughout the entire study period (2010-2022). Having the same taxonomist perform all identifications throughout the study period (2010-2022)
 255 ensures consistency in counting methodology and taxa identification across the time series.

For zooplankton data, initial classification was performed using supervised learning algorithms, followed by expert validation as described in (Irisson et al., 2022). Particularly for samples collected between 2018 and 2023, experts from the PIQv (Quantitative Imaging Platform of Villefranche) reviewed and validated all the already classified objects, making corrections where necessary. This validation process ensured taxonomic homogenization across projects during these years.

260 5 Database structure and analysis

Both monitoring programs show increased complexity over time, evolving from sporadic sampling in 2010-2011 to more systematic seasonal coverage in recent years (Fig. 2). This temporal heterogeneity in sampling effort should be considered when interpreting long-term trends in plankton communities from this dataset.

5.1 Database structure

265 The dataset contains three distinct tables all containing both text and numerical data. The first dataset integrates zooplankton measurements with their corresponding environmental parameters and is organized as follows:

- Metadata information (columns 1-8):
 - Station name (column 1)
 - Transect name (column 2)
 - Coordinates: longitude and latitude (columns 3-4, in DD.dddd)
 - Sampling time: date, year, month, and julian day (columns 5-8)
- Environmental measurements:
 - Surface and bottom temperature (columns 9-10, in °C)
 - Surface and bottom salinity (columns 11-12, in PSU)
- Biological data for each taxonomic group:



- Sample abundance in individuals/m³ (columns 13-116, prefix "conc_" + taxa name)
- Total biovolume in mm³/m³ (columns 117-220, prefix "tot_biov_" + taxa name)
- Mean individual biovolume in mm³ (columns 221-324, prefix "mean_biov_" + taxa name)

The second dataset contains phytoplankton data and follows a similar organizational structure:

- 280 ● Metadata information (columns 1-8):
 - Station name (column 1)
 - Transect name (column 2)
 - Coordinates: longitude and latitude (columns 3-4, in DD.dddd)
 - Sampling time: date, year, month, and julian day (columns 5-8)
- 285 ● Environmental measurements:
 - Surface and bottom temperature (columns 9-10, in °C)
 - Surface and bottom salinity (columns 11-12, in PSU)
- Phytoplankton taxa concentrations:
 - 290 ○ Surface abundance in individuals/L (columns 13-580, prefix "surface_" + taxa name)
 - Bottom abundance in individuals/L (columns 581-1148, prefix "bottom_" + taxa name)

The complete taxonomic hierarchy for each phytoplanktonic taxon, from kingdom to its identification level, was retrieved using the *worms* R-package (Chamberlain and Vanhoorne., 2023). Each taxa is provided in the third dataset with the corresponding unique identifier called *aphiaID* from the World Register of Marine Species (WoRMS Editorial Board, 2025), which enables unambiguous species identification across databases.

295 5.2 Phytoplankton distribution

Figure 4 illustrates both spatial and temporal dynamics of phytoplankton mean absolute abundance across the sampling area. The absolute abundance shows substantial temporal and spatial variability throughout the study period. Notable peaks in total phytoplankton abundance occurred in 2011 and 2022 in the upper panel, with mean abundances exceeding 2×10^6 cells/L at some stations. In the lower panel, remarkable abundance peaks were observed in 2016 and 2021-2022, where mean abundances also exceeded 2×10^6 cells/L.

Interestingly, there does not appear to be a consistent coastal-to-offshore gradient in phytoplankton abundance throughout the years in either northern and southern stations.



305 **Figure 4: Mean absolute abundance (individuals/L) of phytoplankton phyla at surface sampling stations across two**
transects (B on top and D on the bottom) as well as at Molène and Sein coastal stations from 2010 to 2022. Each
 stacked bar represents the total community count at a sampling station, with different colours indicating the absolute
 abundance of each phylum. The upper panel displays the B transect (B1-B7) and the Molène coastal station, while the lower
 panel shows the D transect (D1-D6) and the Sein coastal station. Each phylum is represented by a distinct colour as shown in
 310 the legend.

To have a better look at the composition, we can observe phytoplankton relative abundance as presented in Figure 5. The
 composition shows both temporal variations across years and spatial variations along each transect. Several groups dominate
 the community structure across stations and years, including Cryptophyta (in orange), Heterokontophyta (in dark green),
 315 Myxozoa (in light green) and Nanoflagellates (in light brown). Nanoflagellates are one of the predominant groups in all the
 years except for 2018 and 2019 where they are present in very low proportion. Some groups, such as Cyanobacteria,
 nanophytoplankton and Euglenozoa, appear sporadically and in lower proportions.

Some years present a coast-open ocean gradient in community composition, but most years don't present a clear pattern of
 distribution (Fig. 5). The two coastal stations of Molène and Sein sometimes display a very different distribution. This is
 320 especially visible for the station Sein that presents a high to low presence of cyanobacteria from 2013 to 2016.

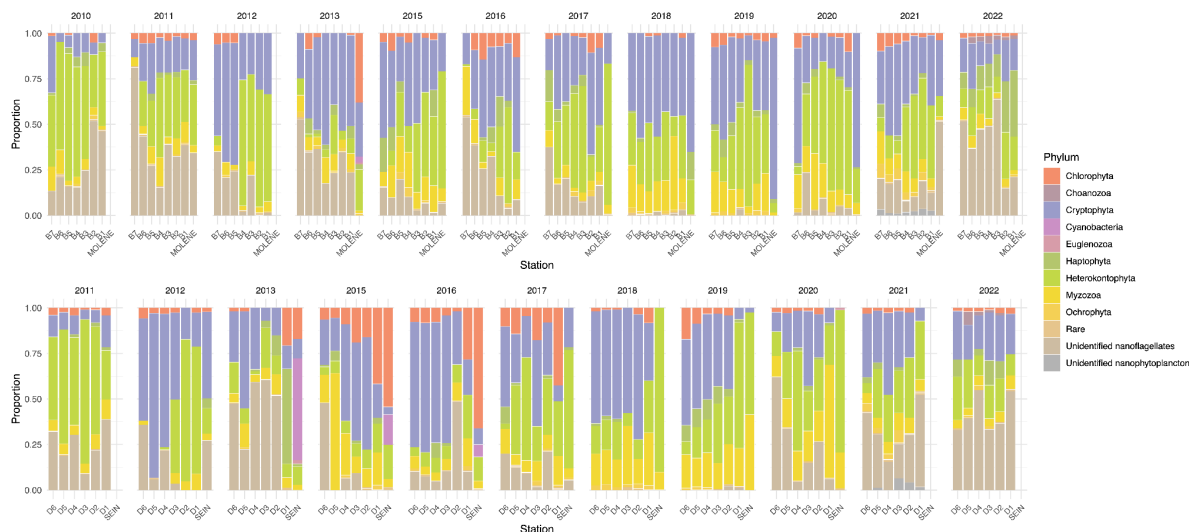


Figure 5: Relative abundance (% of total individuals) of phytoplankton phyla at surface sampling stations across two transects (B on top and D on the bottom) as well as at Molene and Sein coastal stations from 2010 to 2022. The figure shows the proportional composition based on total abundance of phytoplankton at each station. Each stacked bar represents the community composition at a sampling station, with the proportion of each phylum calculated as the percentage of the total abundance of individuals counted at that station. The upper panel displays the B transect (B1-B7) and the Molène coastal station, while the lower panel shows the D transect (D1-D6) and the Sein coastal station from. Each phylum is represented by a distinct colour.

5.3 Zooplankton distribution

Zooplankton data collected from 2010 to 2023 revealed a pronounced coastal-offshore gradient in mean absolute abundance throughout the years (Fig. 6), with decreasing zooplankton concentrations as distance from the coastline increased. Coastal stations (especially B1 and D1) consistently exhibited the highest values, with maximum values reaching up to 6×10^3 individuals per m^3 during peak periods in the transect D. Notably, the D transect stations exhibited abundance values exceeding 2×10^3 individuals per m^3 more frequently than stations along transect B.

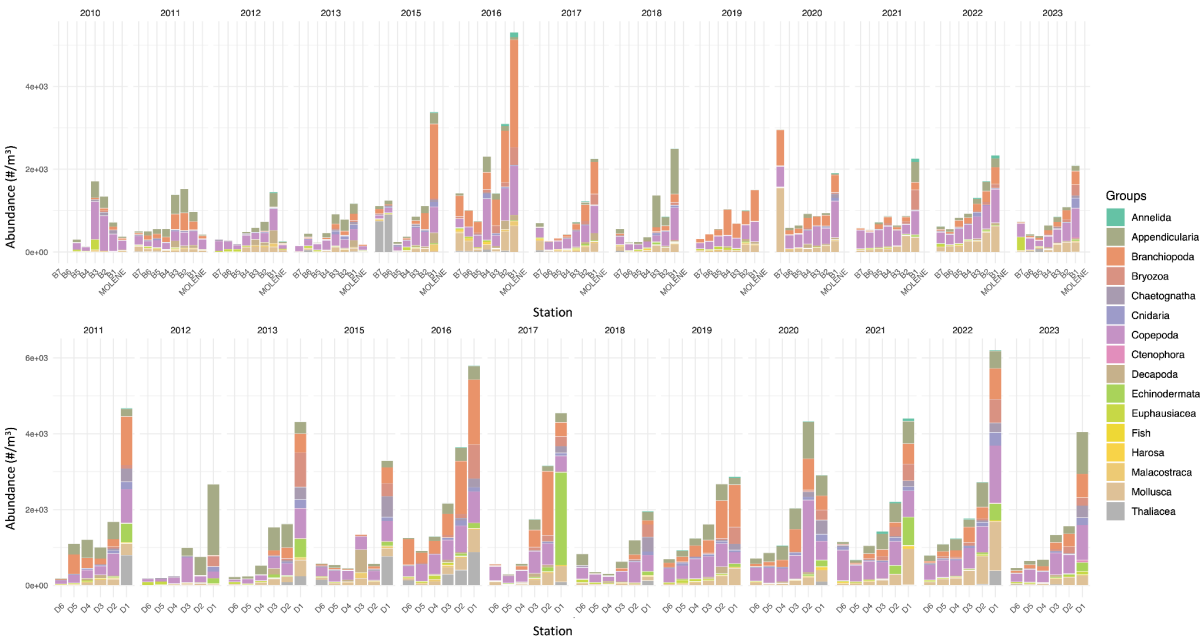


Figure 6: Mean absolute abundance (individuals/m³) of zooplankton phyla at surface sampling stations across two transects (B on top and D on the bottom) and at Molene coastal station from 2010 to 2023. Each stacked bar represents the mean absolute abundance at a specific station, with different colours indicating distinct taxonomic groups as shown in the legend. The upper panel shows data from the B transect (stations B1-B7) and Molene station, while the lower panel displays data from the D transect (stations D1-D6). Note that the Cumacea group was excluded as it only contains 3 images.

The zooplankton community shows clear spatial gradients in dominant groups (Fig. 7). Copepoda exhibits a pronounced coastal-oceanic gradient, with higher proportions in coastal stations decreasing towards open ocean stations. Branchiopoda follows a similar pattern. Conversely, Mollusca shows an inverse gradient with higher proportions at open ocean stations compared to coastal areas. The southern transect (D) is characterized by notably higher proportions of Appendicularia compared to the northern transect. Overall, the community structure remains relatively consistent over the 13-year study period across both transects, suggesting a relatively stable ecosystem structure in the region.

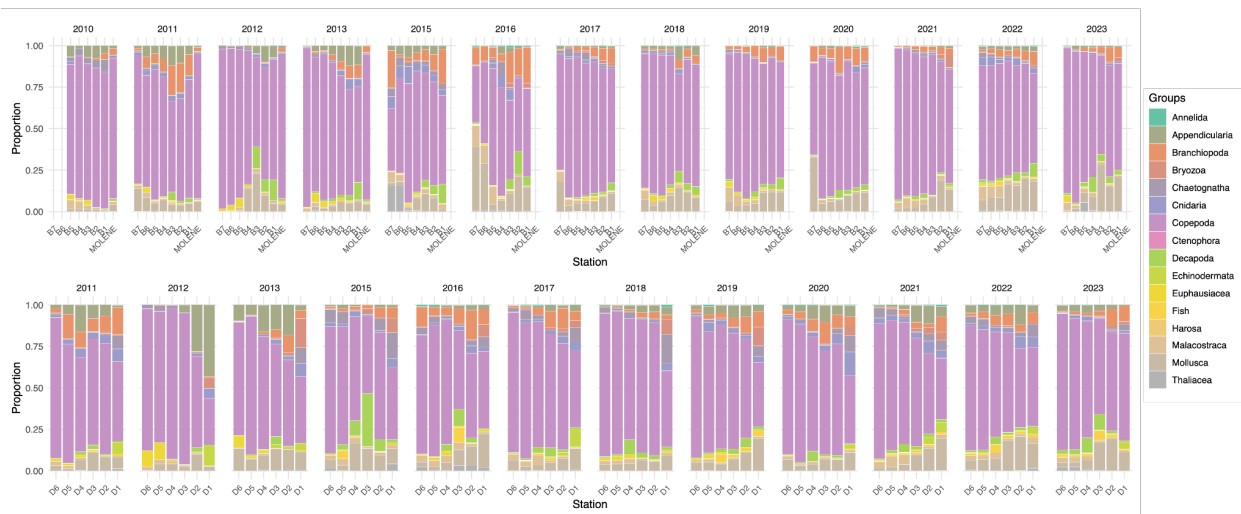


Figure 7: Relative abundance (% of total individuals) of the 16 zooplankton taxonomic groups across two transects (B on top and D on the bottom) and at Molene coastal station from 2010 to 2023. The figure shows the proportional composition based on total counts of zooplankton at each station. Each stacked bar represents the community composition at a sampling station, with the proportion of each phylum calculated as the percentage of the total number of individuals counted at that station. Note that the Cumacea group was excluded as it only contains 3 images. The figure is organized in stacked bar plots showing the proportional composition of the main zooplanktonic groups, with each bar representing a sampling station. The upper panel displays the B transect (B1-B7) and the Molène coastal station, while the lower panel shows the D transect (D1-D6). Each faunistical group is represented by a distinct colour.

6. Concluding remarks

Recent studies have shown significant changes in small pelagic fish communities across French waters, particularly regarding decreases in mean body size and condition (Menu et al., 2023; Queiros et al., 2019), highlighting the critical importance of long-term monitoring of plankton communities (Holland et al., 2025) which constitute their primary food resource (Brosset et al., 2016; Sommer et al., 2018).

The combined physical and biological data enables tracking ecosystem responses to environmental changes while providing baseline data for assessing ecosystem health in this Marine Protected Area. Beyond its ecological significance, the Iroise Sea and the Iroise Marine Natural Park hold particular importance for France's sardine fishery. The region, with Douarnenez as a historic sardine fishing hub, supports a significant portion of France's pelagic fisheries, particularly for purse seiners. This makes the long-term monitoring of plankton communities crucial not only for biodiversity conservation but also for preserving the economic and cultural heritage that led to its designation as France's first Marine Protected Area.



The consistent phytoplankton identification by a single taxonomist throughout the 13-year time series (2010-2022) ensures taxonomic continuity and reliability, providing a robust foundation for studying long-term changes in phytoplankton community structure. The high taxonomic resolution of this dataset (573 distinct phytoplankton taxa across multiple taxonomic levels) enables detailed analyses of phytoplankton community dynamics, biodiversity patterns, and responses to environmental gradients. Additionally, the use of a standardized protocol using the ZooScan imaging system for zooplankton imaging data enables detailed morphometric measurements and creates a standardized visual record, complementing other recently published planktonic datasets that employ various techniques such as microscopy (Acri et al., 2020; Devreker et al., 2024) and imaging instruments (Dugenne et al., 2024; Grandremy et al., 2024). Making such an imaging dataset openly available offers further opportunities for future functional trait-based analyses of plankton dynamics (Litchman et al., 2015; Perhirin et al., 2023; Vilgrain et al., 2021). The plankton communities' descriptors that can be accessed and derived from this dataset (abundances and biovolumes for zooplankton) are proposed at multiple taxonomic levels and accessible through the EcoTaxa web platform (Picheral et al., 2017). These datasets contribute to global plankton monitoring efforts by combining traditional and modern approaches in a standardized format, supporting diverse ecological studies and modeling applications where zooplankton representation has traditionally been simplified usually through size discrimination (Everett et al., 2017). The integration of long-term monitoring and technological innovations strengthens our ability to understand and protect marine ecosystems while providing valuable insights for both immediate research needs and future applications.

7 Data availability

The table containing abundances of phytoplankton and zooplankton as well as zooplankton biovolume are available in the SEANOE data portal: <https://doi.org/10.17882/105465> (Drago et al., 2025). Individual zooplankton images are available to be viewed and explored on the Ecotaxa web application (Picheral et al., 2017, <https://ecotaxa.obs-vlfr.fr/>; no registration needed). The references for the projects are available in Supplementary Table 3.

8 Code availability

Following the FAIR principle (Wilkinson et al., 2016), all code used for data processing and analysis is publicly accessible through our GitHub repository (https://github.com/neccton-algo/PNMI_data_paper).

395 Author contribution

Conceptualization and Methodology: LD, CC, PP, SDA. Data curation and Validation: LD, CC, BB, LJ. Formal analysis, Investigation, Visualization: LD. Funding acquisition: PP, SDA. Project administration and Resources: CC, PP, SDA. Supervision: SDA. Writing – original draft: LD, SDA. Writing – review & editing: LD, CC, PP, BB, LJ, JBR, SDA.



Competing interests

400 The authors declare that they have no conflict of interest.

Disclaimer

While all identifications have been reviewed by at least one human operator, we cannot fully guarantee the correctness of each of the >655k identifications, a few mistakes might remain.

Acknowledgements

405 Co-authors wish to thank French and European public taxpayers who fund their salaries. The authors thank the European Marine Biological Resource Centre (EMBRC) platform PIQv (Quantitative Imaging Platform of Villefranche-sur-Mer) for image analysis. This work was also supported by EMBRC France, whose French state funds are managed by the French National Research Agency within the Investments of the Future program under reference ANR-10-INBS-02. We extend our sincere gratitude to all field crew members of the OFB-PNMI who assisted with sample collection in sometimes very
 410 challenging weather conditions. We also thank Lars Stemmann from Sorbonne University for his help in convincing the OFB-PNMI that it was worth pursuing the plankton sampling during 2014 because of its interest for the scientific community. We also thank everyone who contributed to sample collection and data processing all along the years, making this dataset possible.

Funding sources

415 LD's post-doc is funded by Horizon Europe RIA under Grant Number 101081273 (NECCTON project). SDA acknowledges additional funding by the Institut Universitaire de France and by the French Agence Nationale de la Recherche (ANR), under grant ANR-22-CE02-0023-1 (project TRAITZOO).

References

- 420 Acri, F., Bastianini, M., Bernardi Aubry, F., Camatti, E., Boldrin, A., Bergami, C., Cassin, D., De Lazzari, A., Finotto, S., Minelli, A., Oggioni, A., Pansera, M., Sarretta, A., Socal, G., Pugnetti, A., 2020. A long-term (1965–2015) ecological marine database from the LTER-Italy Northern Adriatic Sea site: plankton and oceanographic observations. *Earth Syst. Sci. Data* 12, 215–230. <https://doi.org/10.5194/essd-12-215-2020>
- 425 Ayata, S.-D., Lazure, P., Thiébaud, É., 2010. How does the connectivity between populations mediate range limits of marine invertebrates? A case study of larval dispersal between the Bay of Biscay and the English Channel (North-East Atlantic). *Prog. Oceanogr.* 87, 18–36. <https://doi.org/10.1016/j.pocean.2010.09.022>



- Batchelder, H.P., Mackas, D.L., O'Brien, T.D., 2012. Spatial–temporal scales of synchrony in marine zooplankton biomass and abundance patterns: A world-wide comparison. *Prog. Oceanogr.*, Global Comparisons of Zooplankton Time Series 97–100, 15–30. <https://doi.org/10.1016/j.pocean.2011.11.010>
- 430 Batten, S.D., Abu-Alhija, R., Chiba, S., Edwards, M., Graham, G., Jyothibabu, R., Kitchener, J.A., Koubbi, P., McQuatters-Gollop, A., Muxagata, E., Ostle, C., Richardson, A.J., Robinson, K.V., Takahashi, K.T., Verheye, H.M., Wilson, W., 2019. A Global Plankton Diversity Monitoring Program. *Front. Mar. Sci.* 6. <https://doi.org/10.3389/fmars.2019.00321>
- 435 Benedetti, F., Jalabert, L., Sourisseau, M., Becker, B., Cailliau, C., Desnos, C., Elineau, A., Irisson, J.-O., Lombard, F., Picheral, M., Stemmann, L., Pouline, P., 2019. The Seasonal and Inter-Annual Fluctuations of Plankton Abundance and Community Structure in a North Atlantic Marine Protected Area. *Front. Mar. Sci.* 6, 214. <https://doi.org/10.3389/fmars.2019.00214>
- Berline, L., Siokou-Frangou, I., Marasović, I., Vidjak, O., Fernández de Puelles, M.L., Mazzocchi, M.G., Assimakopoulou, G., Zervoudaki, S., Fonda-Umani, S., Conversi, A., Garcia-Comas, C., Ibanez, F., Gasparini, S., Stemmann, L., Gorsky, G., 2012. Intercomparison of six Mediterranean zooplankton time series. *Prog. Oceanogr.*, Global Comparisons of Zooplankton Time Series 97–100, 76–91. <https://doi.org/10.1016/j.pocean.2011.11.011>
- 440 Berthou, P., Masse, J., Duhamel, E., Begot, E., Laurans, M., Biseau, A., Pitel-Roudaut, M., Duhamel, E., Begot, E., Laurans, M., Biseau, A., Pitel-Roudaut, M., 2010. La pêche de bolinche dans le périmètre du parc naturel marin d'Iroise.
- Bolaños, L.M., Karp-Boss, L., Choi, C.J., Worden, A.Z., Graff, J.R., Haëntjens, N., Chase, A.P., Della Penna, A., Gaube, P., Morison, F., Menden-Deuer, S., Westberry, T.K., O'Malley, R.T., Boss, E., Behrenfeld, M.J., Giovannoni, S.J., 445 2020. Small phytoplankton dominate western North Atlantic biomass. *ISME J.* 14, 1663–1674. <https://doi.org/10.1038/s41396-020-0636-0>
- Brosset, P., Le Bourg, B., Costalago, D., Bănar, D., Van Beveren, E., Bourdeix, J., Fromentin, J., Ménard, F., Saraux, C., 2016. Linking small pelagic dietary shifts with ecosystem changes in the Gulf of Lions. *Mar. Ecol. Prog. Ser.* 554, 157–171. <https://doi.org/10.3354/meps11796>
- 450 Buitenhuis, E.T., Vogt, M., Moriarty, R., Bednaršek, N., Doney, S.C., Leblanc, K., Le Quéré, C., Luo, Y.-W., O'Brien, C., O'Brien, T., Peloquin, J., Schiebel, R., Swan, C., 2013. MAREDAT: towards a world atlas of MARine Ecosystem DATA. *Earth Syst. Sci. Data* 5, 227–239. <https://doi.org/10.5194/essd-5-227-2013>
- 455 Cadier, M., Sourisseau, M., Gorgues, T., Edwards, C.A., Memery, L., 2017. Assessing spatial and temporal variability of phytoplankton communities' composition in the Iroise Sea ecosystem (Brittany, France): A 3D modeling approach. *J. Mar. Syst.* 169, 111–126. <https://doi.org/10.1016/j.jmarsys.2017.01.004>
- Chamberlain, S., Vanhoorne, B., 2023. worms: World register of marine species (WoRMS) client (manual).
- 460 Chavez, F.P., Bertrand, A., Guevara-Carrasco, R., Soler, P., Csirke, J., 2008. The northern Humboldt Current System: Brief history, present status and a view towards the future. *Prog. Oceanogr.* 79, 95–105. <https://doi.org/10.1016/j.pocean.2008.10.012>
- Cocquempot, L., Delacourt, C., Paillet, J., Riou, P., Aucan, J., Castelle, B., Charria, G., Claudet, J., Conan, P., Coppola, L., Hocdé, R., Planes, S., Raimbault, P., Savoye, N., Testut, L., Vuillemin, R., 2019. Coastal Ocean and Nearshore Observation: A French Case Study. *Front. Mar. Sci.* 6, 324. <https://doi.org/10.3389/fmars.2019.00324>
- 465 Devreker, D., Wacquet, G., Lefebvre, A., 2024. A 45-year hydrological and planktonic time series in the South Bight of the North Sea. <https://doi.org/10.5194/essd-2024-479>
- Drago, L., Cailliau, C., Pouline, P., Beker, B., Jalabert, L., Romagnan, J.-B., Ayata, S.-D., 2025. Plankton and environmental monitoring dataset from the Iroise Marine Natural Park (NE Atlantic, 2010-2023). <https://doi.org/10.17882/105465>
- Drago, L., Panaiotis, T., Irisson, J.-O., Babin, M., Biard, T., Carlotti, F., Coppola, L., Guidi, L., Hauss, H., Karp-Boss, L., Lombard, F., McDonnell, A.M.P., Picheral, M., Rogge, A., Waite, A.M., Stemmann, L., Kiko, R., 2022. Global Distribution of Zooplankton Biomass Estimated by In Situ Imaging and Machine Learning. *Front. Mar. Sci.* 9, 894372. <https://doi.org/10.3389/fmars.2022.894372>
- 470 Dugenne, M., Corrales-Ugalde, M., Luo, J.Y., Kiko, R., O'Brien, T.D., Irisson, J.-O., Lombard, F., Stemmann, L., Stock, C., Anderson, C.R., Babin, M., Bhairy, N., Bonnet, S., Carlotti, F., Cornils, A., Crockford, E.T., Daniel, P., Desnos, C., Drago, L., Elineau, A., Fischer, A., Grandrémy, N., Grondin, P.-L., Guidi, L., Guieu, C., Hauss, H., Hayashi, K., Huggett, J.A., Jalabert, L., Karp-Boss, L., Kenitz, K.M., Kudela, R.M., Lescot, M., Marec, C., McDonnell, A., 475



- Mériguet, Z., Niehoff, B., Noyon, M., Panaïotis, T., Peacock, E., Picheral, M., Riquier, E., Roesler, C., Romagnan, J.-B., Sosik, H.M., Spencer, G., Taucher, J., Tilliette, C., Vilain, M., 2024. First release of the Pelagic Size Structure database: global datasets of marine size spectra obtained from plankton imaging devices. *Earth Syst. Sci. Data* 16, 2971–2999. <https://doi.org/10.5194/essd-16-2971-2024>
- 480 Duhamel, E., Laspougeas, C., Fry, A., 2011. Rapport final du programme d'embarquements à bord des bolincheurs travaillant dans le Parc naturel marin d'Iroise.
- Everett, J.D., Baird, M.E., Buchanan, P., Bulman, C., Davies, C., Downie, R., Griffiths, C., Heneghan, R., Kloser, R.J., Laiolo, L., Lara-Lopez, A., Lozano-Montes, H., Matear, R.J., McEnnulty, F., Robson, B., Rochester, W., Skerratt, J., Smith, J.A., Strzelecki, J., Suthers, I.M., Swadling, K.M., van Ruth, P., Richardson, A.J., 2017. Modeling What We Sample and Sampling What We Model: Challenges for Zooplankton Model Assessment. *Front. Mar. Sci.* 4. <https://doi.org/10.3389/fmars.2017.00077>
- 485 Frederiksen, M., Edwards, M., Richardson, A.J., Halliday, N.C., Wanless, S., 2006. From plankton to top predators: bottom-up control of a marine food web across four trophic levels. *J. Anim. Ecol.* 75, 1259–1268. <https://doi.org/10.1111/j.1365-2656.2006.01148.x>
- 490 Garrido, S., Ben-Hamadou, R., Oliveira, P., Cunha, M., Chicharo, M., Van Der Lingen, C., 2008. Diet and feeding intensity of sardine *Sardina pilchardus*: correlation with satellite-derived chlorophyll data. *Mar. Ecol. Prog. Ser.* 354, 245–256. <https://doi.org/10.3354/meps07201>
- Gorsky, G., Ohman, M.D., Picheral, M., Gasparini, S., Stemmann, L., Romagnan, J.-B., Cawood, A., Pesant, S., Garcia-Comas, C., Prejger, F., 2010. Digital zooplankton image analysis using the ZooScan integrated system. *J. Plankton Res.* 32, 285–303. <https://doi.org/10.1093/plankt/fbp124>
- 495 Grandremy, N., Bourriau, P., Daché, E., Danielou, M.-M., Doray, M., Dupuy, C., Forest, B., Jalabert, L., Huret, M., Le Mestre, S., Nowaczyk, A., Petitgas, P., Pineau, P., Rouxel, J., Tardivel, M., Romagnan, J.-B., 2024. Metazoan zooplankton in the Bay of Biscay: a 16-year record of individual sizes and abundances obtained using the ZooScan and ZooCAM imaging systems. *Earth Syst. Sci. Data* 16, 1265–1282. <https://doi.org/10.5194/essd-16-1265-2024>
- 500 Hasle, G.R., 1978. The inverted-microscope method, in: *Phytoplankton Manual*. pp. 88–96.
- Holland, M.M., Artigas, L.F., Atkinson, A., Best, M., Bresnan, E., Devlin, M., Eerkes-Medrano, D., Johansen, M., Johns, D.G., Machairopoulou, M., Pitois, S., Scott, J., Schilder, J., Stern, R., Tait, K., Whyte, C., Widdicombe, C., McQuatters-Gollop, A., 2025. Mind the gap - The need to integrate novel plankton methods alongside ongoing long-term monitoring. *Ocean Coast. Manag.* 107542. <https://doi.org/10.1016/j.ocecoaman.2025.107542>
- 505 Ikeda, T., 1985. Metabolic rates of epipelagic marine zooplankton as a function of body mass and temperature. *Mar. Biol.* 85, pages 1–11.
- Irisson, J.-O., Ayata, S.-D., Lindsay, D.J., Karp-Boss, L., Stemmann, L., 2022. Machine Learning for the Study of Plankton and Marine Snow from Images. *Annu. Rev. Mar. Sci.* 14, annurev-marine-041921-013023. <https://doi.org/10.1146/annurev-marine-041921-013023>
- 510 Jalabert, L., Elineau, A., Brandão, M., Picheral, M., 2024. Zooscan-Zooprocess user manual and procedures at the Quantitative Imaging Platform of Villefranche-sur-Mer (PIQv). <https://doi.org/10.5281/zenodo.13949803>
- Jonkers, L., Meilland, J., Rillo, M.C., de Garidel-Thoron, T., Kitchener, J.A., Kucera, M., 2022. Linking zooplankton time series to the fossil record. *ICES J. Mar. Sci.* 79, 917–924. <https://doi.org/10.1093/icesjms/fsab123>
- Kenitz, K.M., Orenstein, E.C., Roberts, P.L.D., Franks, P.J.S., Jaffe, J.S., Carter, M.L., Barton, A.D., 2020. Environmental drivers of population variability in colony-forming marine diatoms. *Limnol. Oceanogr.* 65, 2515–2528. <https://doi.org/10.1002/lno.11468>
- 515 Kiørboe, T., Visser, A., Andersen, K.H., 2018. A trait-based approach to ocean ecology. *ICES J. Mar. Sci.* 75, 1849–1863. <https://doi.org/10.1093/icesjms/fsy090>
- Le Boyer, A., Cambon, G., Daniault, N., Herbette, S., Le Cann, B., Marié, L., Morin, P., 2009. Observations of the Ushant tidal front in September 2007. *Cont. Shelf Res.* 29, 1026–1037. <https://doi.org/10.1016/j.csr.2008.12.020>
- 520 Le Floch, P., Alban, F., Merzéréaud, M., Duhamel, E., 2020. Identification des points de rupture dans la série longue des productions de sardine en France (1900-2017). *Rev. Déconomie Ind.* 49–78. <https://doi.org/10.4000/rei.9023>
- Litchman, E., de Tezanos Pinto, P., Edwards, K.F., Klausmeier, C.A., Kremer, C.T., Thomas, M.K., 2015. Global biogeochemical impacts of phytoplankton: a trait-based perspective. *J. Ecol.* 103, 1384–1396. <https://doi.org/10.1111/1365-2745.12438>
- 525



- Litchman, E., Ohman, M.D., Kiørboe, T., 2013. Trait-based approaches to zooplankton communities. *J. Plankton Res.* 35, 473–484. <https://doi.org/10.1093/plankt/fbt019>
- Lund, J.W.G., Kipling, C., Le Cren, E.D., 1958. The inverted microscope method of estimating algal numbers and the statistical basis of estimations by counting. *Hydrobiologia* 11, 143–170. <https://doi.org/10.1007/BF00007865>
- 530 Martini, S., Larras, F., Boyé, A., Faure, E., Aberle, N., Archambault, P., Bacouillard, L., Beisner, B.E., Bittner, L., Castella, E., Danger, M., Gauthier, O., Karp-Boss, L., Lombard, F., Maps, F., Stemmann, L., Thiébaud, E., Usseglio-Polatera, P., Vogt, M., Laviale, M., Ayata, S.-D., 2021. Functional trait-based approaches as a common framework for aquatic ecologists. *Limnol. Oceanogr.* 66, 965–994. <https://doi.org/10.1002/lno.11655>
- 535 Menu, C., Pecquerie, L., Bacher, C., Doray, M., Hattab, T., Van Der Kooij, J., Huret, M., 2023. Testing the bottom-up hypothesis for the decline in size of anchovy and sardine across European waters through a bioenergetic modeling approach. *Prog. Oceanogr.* 210, 102943. <https://doi.org/10.1016/j.pocean.2022.102943>
- Motoda, S., 1959. Devices of Simple Plankton Apparatus. *Mem. Fac. Fish. Hokkaido Univ.*
- Orenstein, E.C., Ayata, S., Maps, F., Becker, É.C., Benedetti, F., Biard, T., De Garidel-Thoron, T., Ellen, J.S., Ferrario, F., Giering, S.L.C., Guy-Haim, T., Hoebeke, L., Iversen, M.H., Kiørboe, T., Lalonde, J., Lana, A., Laviale, M., 540 Lombard, F., Lorimer, T., Martini, S., Meyer, A., Möller, K.O., Niehoff, B., Ohman, M.D., Pradalier, C., Romagnan, J., Schröder, S., Sonnet, V., Sosik, H.M., Stemmann, L.S., Stock, M., Terbiyik-Kurt, T., Valcárcel-Pérez, N., Vilgrain, L., Wacquet, G., Waite, A.M., Irisson, J., 2022. Machine learning techniques to characterize functional traits of plankton from image data. *Limnol. Oceanogr.* 67, 1647–1669. <https://doi.org/10.1002/lno.12101>
- 545 Panaïotis, T., Babin, M., Biard, T., Carlotti, F., Coppola, L., Guidi, L., Hauss, H., Karp-Boss, L., Kiko, R., Lombard, F., McDonnell, A.M.P., Picheral, M., Rogge, A., Waite, A.M., Stemmann, L., Irisson, J., 2023. Three major mesoplanktonic communities resolved by in situ imaging in the upper 500 m of the global ocean. *Glob. Ecol. Biogeogr.* geb.13741. <https://doi.org/10.1111/geb.13741>
- Perhirin, M., Gossner, H., Godfrey, J., Johnson, R., Blanco-Bercial, L., Ayata, S., 2023. Morphological and taxonomic diversity of mesozooplankton is an important driver of carbon export fluxes in the ocean. *Mol. Ecol. Resour.* 24, e13907. <https://doi.org/10.1111/1755-0998.13907>
- 550 Picheral, M., Colin, S., Irisson, J.-O., 2017. EcoTaxa, a tool for the taxonomic classification of images.
- Pingree, R.D., Pugh, P.R., Holligan, P.M., Forster, G.R., 1975. Summer phytoplankton blooms and red tides along tidal fronts in the approaches to the English Channel. *Nature* 258, 672–677. <https://doi.org/10.1038/258672a0>
- 555 Pitois, S., Yebra, L., 2022. Contribution of marine zooplankton time series to the United Nations Decade of Ocean Science for Sustainable Development. *ICES J. Mar. Sci.* 79, 722–726. <https://doi.org/10.1093/icesjms/fsac048>
- Queiros, Q., Fromentin, J.-M., Gasset, E., Dutto, G., Huiban, C., Metral, L., Leclerc, L., Schull, Q., McKenzie, D.J., Saraux, C., 2019. Food in the Sea: Size Also Matters for Pelagic Fish. *Front. Mar. Sci.* 6, 385. <https://doi.org/10.3389/fmars.2019.00385>
- 560 Ramond, P., Siano, R., Schmitt, S., De Vargas, C., Marié, L., Memery, L., Sourisseau, M., 2021. Phytoplankton taxonomic and functional diversity patterns across a coastal tidal front. *Sci. Rep.* 11, 2682. <https://doi.org/10.1038/s41598-021-82071-0>
- Richardson, A.J., Bakun, A., Hays, G.C., Gibbons, M.J., 2009. The jellyfish joyride: causes, consequences and management responses to a more gelatinous future. *Trends Ecol. Evol.* 24, 312–322. <https://doi.org/10.1016/j.tree.2009.01.010>
- 565 Schultes, S., Sourisseau, M., Le Masson, E., Lunven, M., Marié, L., 2013. Influence of physical forcing on mesozooplankton communities at the Ushant tidal front. *J. Mar. Syst.* 109–110, S191–S202. <https://doi.org/10.1016/j.jmarsys.2011.11.025>
- Simon, N., Cras, A.-L., Foulon, E., Lemée, R., 2008. Diversity and evolution of marine phytoplankton. *C. R. Biol.* 332, 159–170. <https://doi.org/10.1016/j.crv.2008.09.009>
- 570 Sommer, U., Charalampous, E., Scotti, M., Moustaka-Gouni, M., 2018. Big fish eat small fish: implications for food chain length? *Community Ecol.* 19, 107–115. <https://doi.org/10.1556/168.2018.19.2.2>
- Sonnet, V., Guidi, L., Mouw, C.B., Puggioni, G., Ayata, S.-D., 2022. Length, width, shape regularity, and chain structure: time series analysis of phytoplankton morphology from imagery. *Limnol. Oceanogr.* 67, 1850–1864. <https://doi.org/10.1002/lno.12171>
- 575 Steinberg, Landry, M.R., 2017. Zooplankton and the Ocean Carbon Cycle. *Annu. Rev. Mar. Sci.* 9, 413–444. <https://doi.org/10.1146/annurev-marine-010814-015924>



- Titocci, J., Pata, P.R., Durazzano, T., Ayata, S.-D., Clerc, C., Cornils, A., Duffy, P., Greer, A.T., Halsband, C., Heneghan, R.F., Lacoursière-Roussel, A., Lombard, F., Majaneva, S., Pakhomov, E.A., Reis, C., Rist, S., Rommel, A.C.M., Silva, T., Stemmann, L., Ugwu, K., Basset, A., Rosati, I., Murphy, K.J., Hunt, B.P.V., 2025. Pathways for converting zooplankton traits to ecological insights are paved with findable, accessible, interoperable, and reusable (FAIR) data practices. ICES J. Mar. Sci. 82, fsaf017. <https://doi.org/10.1093/icesjms/fsaf017>
- 580 van der Lingen, C., Hutchings, L., Field, J., 2006. Comparative trophodynamics of anchovy *Engraulis encrasicolus* and sardine *Sardinops sagax* in the southern Benguela: are species alternations between small pelagic fish trophodynamically mediated? Afr. J. Mar. Sci. 28, 465–477. <https://doi.org/10.2989/18142320609504199>
- 585 Vandromme, P., Stemmann, L., Garcia-Comas, C., Berline, L., Sun, X., Gorsky, G., 2012. Assessing biases in computing size spectra of automatically classified zooplankton from imaging systems: A case study with the ZooScan integrated system. Methods Oceanogr. 1–2, 3–21. <https://doi.org/10.1016/j.mio.2012.06.001>
- Vilgrain, L., Maps, F., Picheral, M., Babin, M., Aubry, C., Irisson, J., Ayata, S., 2021. Trait-based approach using in situ copepod images reveals contrasting ecological patterns across an Arctic ice melt zone. Limnol. Oceanogr. 66, 1155–1167. <https://doi.org/10.1002/lno.11672>
- 590 Wilkinson, M.D., Dumontier, M., Aalbersberg, I.J., Appleton, G., Axton, M., Baak, A., Blomberg, N., Boiten, J.-W., Da Silva Santos, L.B., Bourne, P.E., Bouwman, J., Brookes, A.J., Clark, T., Crosas, M., Dillo, I., Dumon, O., Edmunds, S., Evelo, C.T., Finkers, R., Gonzalez-Beltran, A., Gray, A.J.G., Groth, P., Goble, C., Grethe, J.S., Heringa, J., 'T Hoen, P.A.C., Hooft, R., Kuhn, T., Kok, R., Kok, J., Lusher, S.J., Martone, M.E., Mons, A., Packer, A.L., Persson, B., Rocca-Serra, P., Roos, M., Van Schaik, R., Sansone, S.-A., Schultes, E., Sengstag, T., Slater, T., Strawn, G., Swertz, M.A., Thompson, M., Van Der Lei, J., Van Mulligen, E., Velterop, J., Waagmeester, A., Wittenburg, P., Wolstencroft, K., Zhao, J., Mons, B., 2016. The FAIR Guiding Principles for scientific data management and stewardship. Sci. Data 3, 160018. <https://doi.org/10.1038/sdata.2016.18>
- 595 WoRMS Editorial Board, 2025. World Register of Marine Species. <https://doi.org/10.14284/170>